Scientific Research Publishing

Journal of Materials Science and Chemical Engineering, 2024, 12, 54-66
https://www.scirp.org/journal/msce
ISSN Online: 2327-6053
ISSN Print: 2327-6045

Electrochemical Studies on Photoactive Thin Solid Films of Poly (2-(2-Thienyl) Furan) Occluded with a g-C_3N_4/SiC Mixture in Gel Electrolyte

Kasem K. Kasem*, Joe Russeau

School of Sciences, Indiana University Kokomo, Kokomo, USA
Email: *kkasem@iu.edu

How to cite this paper: Kasem, K.K. and Russeau, J. (2024) Electrochemical Studies on Photoactive Thin Solid Films of Poly (2-(2-Thienyl) Furan) Occluded with a g-C_3N_4/SiC Mixture in Gel Electrolyte. *Journal of Materials Science and Chemical Engineering*, **12**, 54-66.
https://doi.org/10.4236/msce.2024.1212004

Received: November 1, 2024
Accepted: December 8, 2024
Published: December 11, 2024

Abstract

Photoactive assemblies were created using SiC, C_3N_4 (CN), and Poly (2-(2-thienyl) furan) (PTF). These assemblies underwent spectroscopic and photoelectrochemical (PEC) investigations. The results show that these ternary semiconductor assemblies combine the advantages of each component to produce an enhanced photo response outcome. As a multiphase photocatalyst, they minimize or eliminate the electron-hole fast recombination problems associated with single-phase assemblies. Spectroscopic studies indicate that all assembly components absorb visible light photons with energy between 3.1 and 2.1 eV. The largest PEC photo response outcome was recorded when PTF was occluded with each SiC, CN, or both. PEC studies show that PTF/SiC/CN generates greater photon-to-charge conversion than PTF/SiC or PTF/CN. The photodiode parameters of the PTF/SiC/CN were calculated. The ideality factor was >1, which is expected from organic polymer semiconductors. The obtained spectroscopic/PEC results were explained by suggesting that PTF creates a better environment for forming multiphase interfaces to facilitate the movement of charge carriers and prevent the recombination of electron-hole pairs.

Keywords

Electrochemistry, Organic Semiconductors, Gel Electrolyte, Photocurrent, Multiphase Assemblies

1. Introduction

The proven photocatalytic capabilities of graphite carbon nitride g-C_3N_4 or (CN) for hydrogen evolution in aqueous electrolytes under visible light irradiation

attracted the attention of many research efforts [1]-[5]. g-C_3N_4 as a polymeric graphite-like photocatalyst has great physicochemical stability. Further, SiC is a typical non-metallic semiconductor with some photocatalytic activities with good physicochemical stability. Several investigations highlighted the photocatalytic reactions of SiC alone or combined with other photoactive materials [6]-[10]. SiC- or CN-based assemblies are single-phase photocatalysts. Some problems with single-phase photocatalysts, such as electron-hole fast recombination and low photocatalyst capabilities, limit their use. On the other hand, a binary or multiple system, with a suitable band structure, can create a smooth phase interface that enhances charge carriers' transfer in opposite directions of these interfaces. An assembly consisting of both (SiC and CN) can overcome the limitations mentioned above of single-phase assemblies.

Both materials are important because of their moderate band gap value, which allows them to harvest visible light radiation. The reported band gaps are between 2 and 3 eV. Harvesting solar energy can be enhanced by forming heterojunction systems of semiconductors with band gaps within the visible solar spectrum. SiC shares some similarities with graphene, however, in SiC alternating Si atoms with carbon atoms in a planer hexagonal structure generates different properties such as conductivity, thermal stabilities, and other physical properties. Furthermore, CN also possesses a graphene-type structure. The π bond conjugation in their structure gives rise to the semi-conductivity properties and the moderate band gap values. Previous studies [11]-[14] investigated using mixtures of CN/SiC in aqueous electrolytes. Most of the mentioned studies highlighted the proven capabilities of both SiC and CN for removing contaminants and excellent chemical stabilities in both aqueous and organic solvents. The lack of studies on the behavior of these combined semiconductors immobilized into photoactive organic polymers raises the interest in examining their behavior in gel electrolytes (GE).

This study focused on evaluating the photoelectrochemical (PEC) responses of a ternary system composed of SiC, CN, and PTF (as conjugated organic polymer) in assembly (CN/SIC/PTF). The goal is to see if PTF provides a better environment to create multiphase interfaces that facilitate charge carrier movements with both CN and SiC and prevent the recombination of e/h pairs.

2. Experimental

All materials used were of analytical grade. 2(2-thienyl) furan (TF) was used as received from Aldrich Co.

2.1. Instrumentation

All electrochemical experiments were carried out using either a conventional three-electrode cell or a previously described electrochemical cell [15]. A BAS 100W electrochemical analyzer (Bioanalytical Co.) was used to perform the electrochemical studies such as cyclic voltammetry (CV) and chronoamperometry (CA). Steady-state reflectance spectra were performed using Shimadzu UV-2101

PC. Irradiations were performed with a solar simulator 300-watt xenon lamp with an IR filter (Newport). Electrochemical Impedance spectroscopy (EIS) was carried out using a Solarton 2101A. Photoelectrochemical (PEC) studies of the thin solid films in gel electrolyte were performed using 2.0 cm^2 fluorine-doped Tin Oxide (FTO) covered with the photoactive material as a working electrode, and platinized FTO (Pt-FTO) served as both reference and counter electrode. Unless otherwise stated, all potentials were measured against platinized FTO (0.597 vs. SHE).

2.2. *In-Situ* Formation of CN/SiC/PTF Assembly

A CV in situ technique was used to incorporate SiC or CN nanoparticles, as well as a mixture of both, into PTF. In a typical 2-electrode cell setup, FTO serves as the working electrode, while Pt-FTO functions as both the reference and counter electrode. Subsequent sections will provide more details about the *in-situ* formation of CN/SiC/PTF.

2.3. Preparation of Thermoplastic Gel Electrolyte (TPGE)

Thermoplastic gel electrolyte (TPGE) was prepared following the published procedure [16]. Briefly, 0.65 M KI and 0.065M I_2 were dissolved in 10 mL polycarbonate (PC), and then 8.5 g of PEG (M-20000) was added to the mixture. The mixture was heated at 100˚C under continuous stirring for ca. 12 h in a flask under an inert atmosphere. The mixture was hydrothermally treated at 180˚C for 14 h in a Teflon autoclave.

2.4. Preparation of Gel-Based Electrochemical Cell

A 100 µL of 10 mM monomer solution with or without the SiC or CN was placed onto a rectangular conducting fluorinated Tin oxide glass (FTO) window area of 1.5 cm^2 working electrode. The monomer spread evenly on the electrode surface and further evaporated the solvent. A 200 µL of 1:10 I_2/KI in polyethylene glycol gel electrolyte was placed on the top of the monomer layer. Immediately the counter electrode was placed on top of the gel electrolyte and pressed to allow an even spread of the electrolyte between the two electrodes.

2.5. Measuring PEC Responses of *In-Situ* Monomer/Polymer Transition

The following steps were performed to report the in-situ PEC responses of studied assemblies.

Prepare the EC cell as mentioned in the experimental section.

- Step 1—Run a CV between 0 to −1.4 V vs the Pt-FTO reference electrode was run at a scan rate of 0.1 V/s without illumination (dark). The resulting voltammogram represents the monomer behavior without illumination MD (monomer dark).
- Step 2—Run a CV between 0 to −1.5 V vs the reference electrode at a scan rate of 0.1 V/s. The resulting voltammogram represents the monomer behavior

under illumination ML (monomer light).

- Step 3—Run oxidative Electropolymerization of the monomer at a constant potential of 1.6 V for 10 seconds to ensure complete polymerization of the monomer.
- Step 4—After Step 3 treatment, run a CV between 0 to −1.4 V vs the reference electrode at a scan rate of 0.1 V/s under dark. The resulting voltammogram represents the polymer behavior under dark PD (polymer dark).
- Step 5—Repeat step 4 but under illumination. The resulting voltammogram represents the polymer behavior under illumination P_L (polymer light). The outcome of these steps for each studied assembly generates I-V figures.

Charge involvement for monomer-dark (Q_M-D), monomer-light (Q_M-L), and polymer light (Q_P-L) was calculated by integrating the area of each resultant voltammogram.

"Photocurrent and the resulting photo-generated charges are used to measure photoactivity". Therefore:

- (Q_M-L) − (Q_M-D) = Charge activity of the monomer or (PEC-M)
- (Q_P-L) − (Q_M-D) = Charge activity of the polymer or (PEC-P)
- Q Photo charge due to polymerization = (PEC-P) − (PEC-M).

3. Results and Discussions

3.1. Optical and Spectroscopic Studies

The light absorption of the assembly consisting of PTF/SiC-CN has been examined. The results are presented in **Figure 1** and **Figure 2**. **Figure 1** illustrates the similarities in the absorption pattern of SiC (band gap 2.31 eV) and CN (band gap 2.48 eV). Previous studies [17] have indicated that the spectra of the mixed SiC and CN show a broadening of the light absorption range, suggesting an interaction between the SiC and CN as an active mixture. **Figure 2** shows Tauc plots used to analyze the absorption data presented in **Figure 1**. **Figure 2(A)** suggests that a direct band gap likely exists. The multiple absorption peaks seen in **Figure 1(B)** result from the potential coexistence of various forms of SiC and CN. It should be noted that the absorption edge at 2.3 eV (**Figure 2(B1)**) is for PTF. The presence of multi-absorption peaks for PTF is due to insoluble oligomers within the polymer matrix of PTF. These oligomers absorb higher energy photons.

Figure 1 and **Figure 2** indicate that all components of the assembly PTF/SiC-CN absorb visible light photons. This promotes the additive absorption action which effectively absorbs most of the visible light photons posing energy between 3.1 to 2.1 eV. The multiple absorption peaks for the prepared assemblies indicate the possible formation of hybrid sub-bands. The absorption spectra of the SiC/CN mixture and that of SiC/CN occluded in PTF are displayed in **Figure 3(A)** & **Figure 3(B)** respectively. This figure shows a noticeable shift of absorption edges and peaks of the SiC/CN (**Figure 3(A)** trace 1) from that of SiC/CN /PTF (**Figure 3(A)** trace 2). The addition of PTF causes an increase in absorption at a longer wavelength (red shift). Comparing the absorption profile of each component alone

(Figure 2) and that of the mixed components (Figure 3) shows a similar pattern, however, the absorption spectra of the mixture have the potential of effective absorption of more visible light.

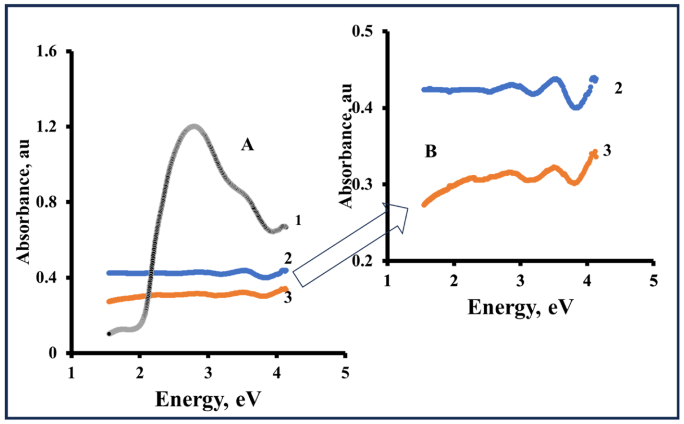

Figure 1. (A) Absorption spectra for 1—PTF, 2—CN, and 3—for SiC, (B) exploded view of absorption spectra of SiC and that of CN.

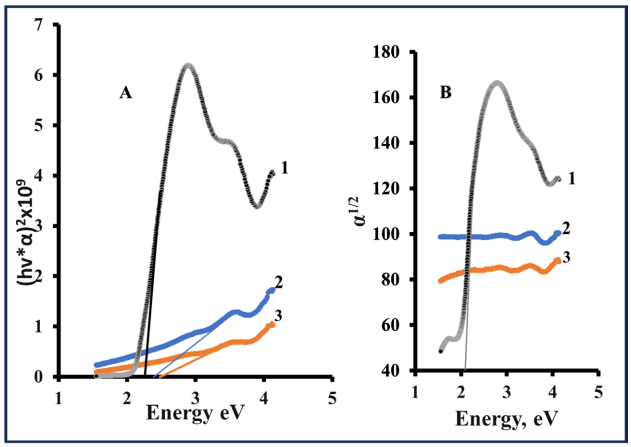

Figure 2. Tauc plots (A) Photon energy vs α^2, (B) Photon energy vs $\alpha^{1/2}$ for 1—PTF, 2—CN, and 3—SiC.

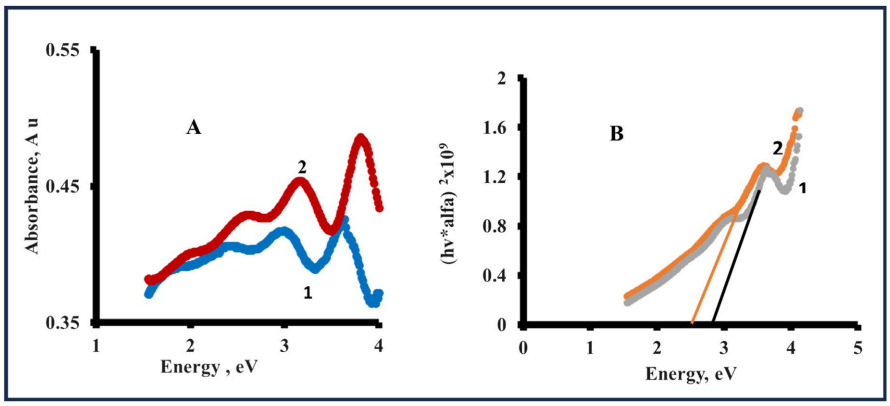

Figure 3. (A) Absorption spectra, (B) Tauc plot for 1—FTO/SiC + C_3N_4, 2—For FTO/SiC + C_3N_4 + PTF.

3.2. Photoelectrochemical Studies

The PEC studies were conducted on FTO/SiC, FTO/CN, FTO/SiC-CN, and FTO/SiC-CN-PTF in the thermoplastic I^-/I_3^- gel electrolyte (TPGE). The studies were conducted in the dark and under illumination, with a scan rate of 0.10 V/s. Some of the CVs are shown in Figures 4-6, while the complete results are listed in Table 1 and Table 2. *In-situ* monomer/polymer transition studies are performed when TF is involved in any process.

3.2.1. PEC of FTO/SIC-CN/PTF in Gel Electrolyte

Figure 4 displays a CV scan for the SiC/CN/PTF in gel electrolyte under dark and illumination. The figure shows that upon illumination, there is an increase in the recorded current in both cathodic and anodic scans. It can be noticed that the current under illumination starts to exceed the current under dark at ≈ 0.2 V vs the reference electrode. This indicates the fermi level ($E_{\text{flat-band}}$) at 5.4 eV on the vacuum scale. Figure 5(A) displays chronoamperometric studies at −1.2 V for SiC/CN/PTF under dark and under illumination. The noticeable gradual increase in photocurrent upon illumination negates the presence of hole accumulation. The shaded area in Figure 5(A) represents the phenomenon known as dark current. Dark current means the assembly photocurrent did not drop suddenly to zero in the absence of illumination but rather gradually decay. The presence of dark current phenomena reflects a random generation of e/h within the depletion region at the FTO/SiC-CN-PTF interface. Figure 5(B) plots Ln R vs time, s to calculate the charge decay time in the absence of illumination. The basic equation [18] for this plot is:

$$R = \mathrm{e}^{-\frac{t}{\tau}}$$

where t is time, τ is the transient time constant, and $R = \left(I_t - I_{st}\right) / \left(I_{in} - I_{st}\right)$, as I_t is current at time t, I_{in} is immediate photocurrent, and I_{st} is the stationary value of photocurrent (steady current). The plot of ln R *vs.* time (Figure 5(B)) generates a straight line with slope = $1/\tau$. The reciprocal of the slope determines the value of τ, in seconds. The calculated τ is ≈ 5.49 seconds.

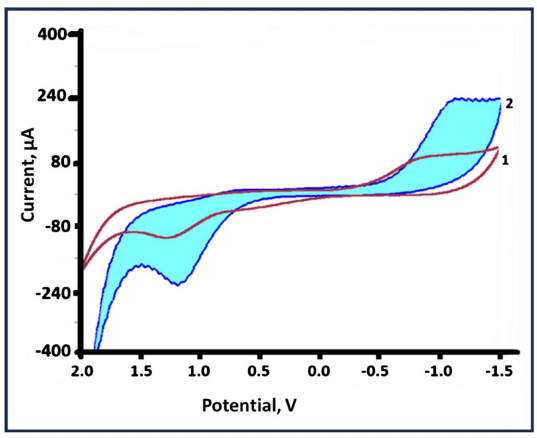

Figure 4. I vs E at scan rate 0.1 V/s in gel electrolyte for FTO/SiC/CN/PTF (1) Dark, (2) under illumination.

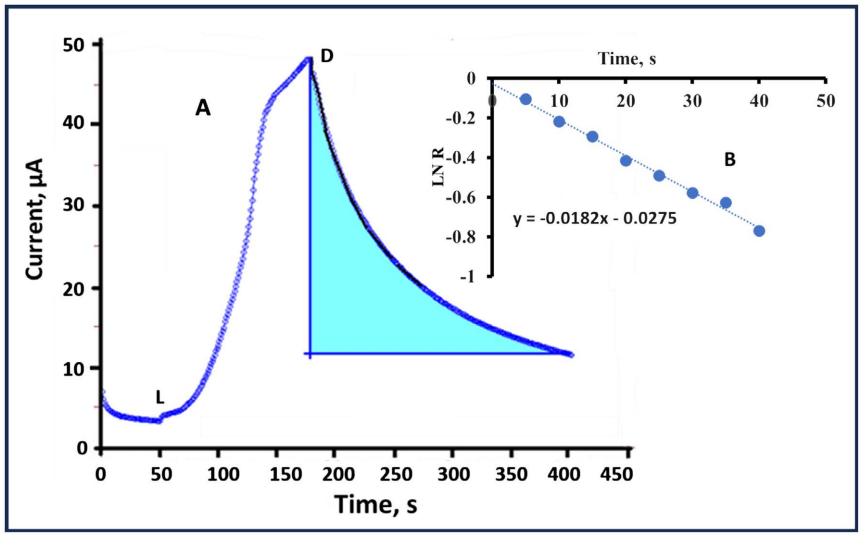

Figure 5. (A) Chronoamperometric studies at −1.2 V vs Ref for FTO/SiC/CN/PTF gel electrolyte, *L* = light, *D* = Dark, (B) Ln R vs Time, s.

3.2.2. PEC of FTO/SiC/CN Only in Gel Electrolyte

The CV scan for the FTO/SiC-CN was not identical but like that shown in Figure 4. However, the magnitude of photocurrent was less than that recorded in the presence of PTF. The study was focused on the potential range between 0 to −1.6 V. Figure 6(A) displays a CV scan for the SiC/CN in gel electrolyte under dark and illumination. The figure shows that upon lighting, there is an increase in the recorded current in both cathodic and anodic scans. It can be noticed that the photocurrent starts to exceed the recorded current (In the dark) at ≈ −0.2 V vs the reference electrode. This shifts the fermi level ($E_{\text{flat-band}}$) at 5.0 eV. This is a shred of evidence that adding PTF alters the energy map structure of the assembly

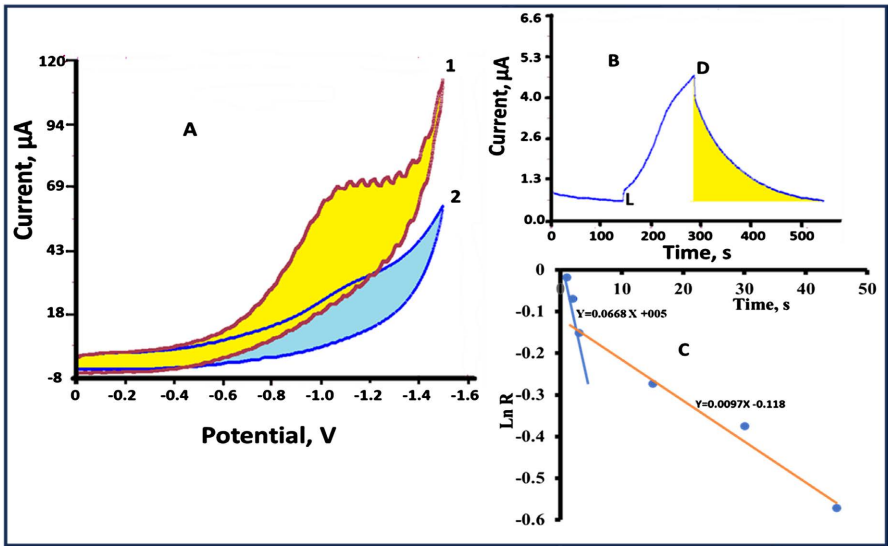

Figure 6. (A) *I* vs *E* at scan rate 0.1 V/s in gel electrolyte for 1—FTO/SiC/CN under illumination, 2—FTO/SiC/CN in the dark, (B) Chronoamperometric studies at −1.2 V vs Ref for FTO/SiC/CN, and (C) plot of Ln R vs time, s. (*L* = light, *D* = Dark).

FTO/SiC/CN. Figure 6(B) displays chronoamperometric studies at −1.2 V for SiC/CN under dark and under illumination. Again, the phenomena of dark currents show up as indicated by the shaded area in Figure 6(B). The calculated transient time constant τ *is* ≈ 100 s (Figure 6(C)). This is much longer than that calculated in the presence of PTF (≈5.49 s). This indicates that PTF creates effective interfaces that facilitate charge carrier movements.

3.2.3. Quantitative Evaluation of PEC Responses of Monomer/Polymer Transition

Following the protocol described in section 2.5, the obtained CV scans were like that displayed in Figure 7. The outcome of these calculations is listed in Table 1.

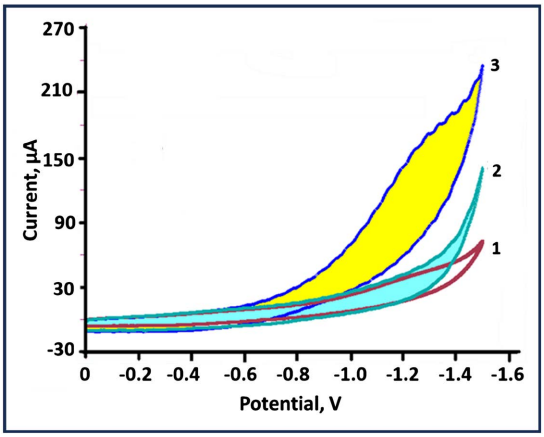

Figure 7. *I* vs *E*. at scan rate 0.1 V/s in gel electrolyte for 1—FTO/SiC + C_3N_4 + TF in dark, 2—FTO/SiC+CN + TF under illumination, 3—FTO/SiC + CN + PTF under illumination.

Table 1. Photon to charge conversion for studied assemblies.

Assembly	*D*, Charge, Q_D, μC	*L*, Charge, Q_L, μC	L occluded Poly. Charge, $QL_{PTF+occluded}$, μC	Difference μC	PTF Effect[a] $QL_{PTF+occluded} - Q_L$ μC
SiC	265.2	402.1		137	
SiC-TF	253.41	405.6	772	366.4	370.3
CN	98.18	133.1		39.0	
TF-CN	265.2	324.3	488.86	164.6	355.76
SiC-CN	189.3	290.7		101.4	
SiC-CN-TF	382.24	456.9	769.43	312.5	478.73

a: SiC, or C_3N_4 or both.

Upon detailed analysis of the data shown in Table 1, the following findings are noticed:

1) The presence of PTF with CN, SiC, and both enhances the photocurrent outcome (approximately 5th column).

2) PTF with a mixture of SiC and CN gives the highest photocurrent (approximately in the 6th column).

3) TF with SiC exhibits a slightly higher increase in the photo response compared to CN.

These findings support the assumption that PTF creates effective interfaces with both SiC and CN that facilitate charge carrier movements. This resulted in a better photo response outcome.

3.2.4. Photodiode Characteristics of the Studied Photoactive Assemblies

Certain photodiode characteristics such as responsivity (R) can be calculated from the ratio of photocurrent and the optical power density of incident light, Detectivity (D) is a measure of the ability of a photodetector to distinguish weak signals from noise, Ideality factor (n) indicates how a diode's current-voltage characteristics closely match an ideal diode, Barrier height (Φ) is the energy barrier at the p-n junction that electrons have to overcome to go through the diode, S (sensitivity of the diode to light) is the ratio of photocurrent to dark current at a given voltage, indicating the ability of the diode to conduct current in one direction compared to the other. The photodiode parameters of the studied photo assemblies FTO/SiC-CN, and FTO/SiC-CN /PTF were determined following the previous work [19] and listed in Table 2.

Table 2. Photodiode parameters of FTO/SiC-CN/Gel/Pt-FTO, and FTO/SiC-CN/PTF/Gel/Pt-FTO.

Assembly	R, responsivity	D Detectivity, jones	n Ideality factor	Φ Barrier height, eV	I_{ph}/I_{dark} S
SiC-C_3N_4/Gel	0.0041	3.39×10^9	18.11	$L = 0.377$ $D = 0.378$	63.8
SiC-C_3N_4/PTF/Gel	0.0122	2.89×10^9	17.38	$L = 0.3505$ $D = 0.366$	16.3

The calculated R, D, and n values for the studied assemblies were closer to that previously calculated [19] for organic photodiodes.

3.2.5. Electrochemical Impedance Spectroscopic Studies

EIS of the FTO/SiC/CN/PTF assembly in gel electrolyte was achieved between 10^5 and 10^{-1} Hz different potentials. Nyquist plot and log σ AC conductivity vs Log frequency generated from this study in the dark and under illumination, are displayed in Figure 8 and Figure 9. Figure 8 shows mainly diffusional control across the studied frequency range. Figure 8(A) indicates that light decreases the film resistance at high frequency as shown from the intercept with the real Z axis. On the other hand, Figure 8(B) shows a kinetic control at high frequency. The illumination does not affect film resistance at high frequencies. At low frequencies the diffusional control is shown under both dark and illumination, however, illumination increases the imaginary impedance. No evidence of charge saturation is reported. The shape of the Nyquist plot with the presence of an un-concentered semicircle at high frequencies

and Warburg impedance at low frequencies (Figure 8(B)) reflects film porosity [20].

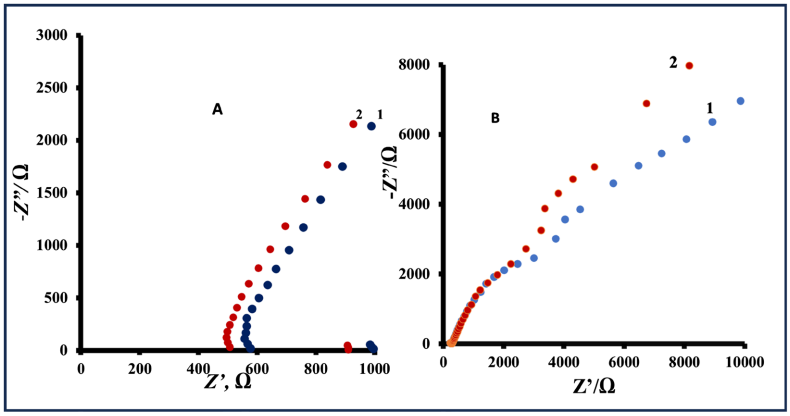

Figure 8. Nyquist plot at (A) 0.0 V, and (B) at −1.0 V vs. platinized FTO for FTO/SiC/CN/PTF (1 = dark, 2 = under illumination).

The plot in Figure 9 shows the relationship between the conductivity (σ) and frequency (ω) for FTO/SiC/CN/PTF in gel electrolyte. The AC conductivity increases with frequency up to approximately 130 Hz. After this point starts to decrease regardless of the applied potential. This is contrary to what was reported previously with FTO/SiC/PTF [21]. The decrease of AC conductivity at frequencies greater than 100 HZ, can be attributed to the presence of CN with SiC occluded in PTF. In assembly FTO/SiC/PTF such behavior was not observed. This suggests that CN, at higher frequencies, affected the mobility of the charge carriers in the applied electric field, resulting in reduced net movement of charge and lower conductivity. Under illumination, no tangible changes in the conductivity compared to that measured in the absence of light. However, at the low-frequency range (ca 0.01 - 10 Hz), the AC conductivity measured at 0.0 (Figure 9(A)) was less than that measured at −1.0 V (Figure 9(B)). This can be explained based on increasing charge carriers at −1.0 V due to the polarization of gel electrolyte's ions at this applied potential.

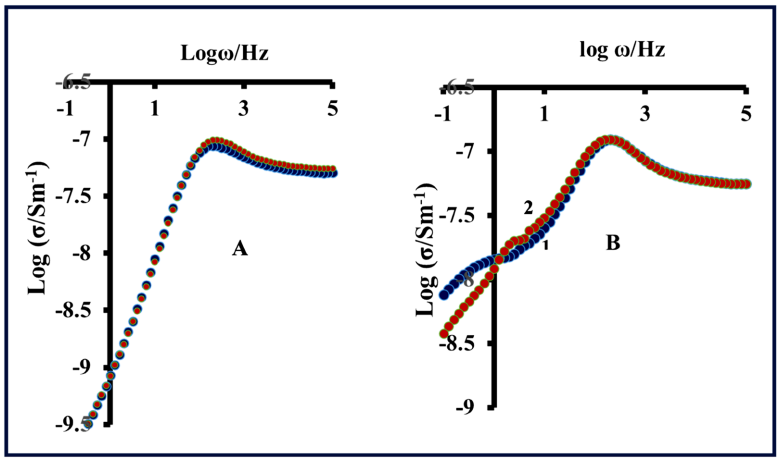

Figure 9. Log electrical conductivity (σ) vs. log frequency (ω) at 0.0 V (A), and at −1.0 V (B) vs. platinized FTO for FTO/SiC/CN/PTF (1 = dark, 2 = under illumination).

4. Conclusion

This study demonstrated that PTF provides a better environment for the creation of multiphase interfaces that facilitate charge carrier movements with both CN and SiC and prevent the recombination of e/h pairs as evident from EC and PEC studies. PEC behavior of SiC/CN particles occluded in PTF in a polyethylene glycol-based gel electrolyte shows that the molecular SiC and CN solid particles have integrated photo activities within the PTF as a host photoactive polymer. CV studies demonstrate a maximum increase in photocurrent when SiC and CN are both included in PTF. This indicates that PTF facilitates the movement of charge carriers. Chronoamperometric studies revealed the presence of dark current phenomena and a lack of hole accumulation upon illumination of FTO/SiC/CN/PTF interfaces. EIS provided evidence of the studied assembly's film porosity. A minor kinetically controlled charge transfer at high frequency and a major diffusional controlled charge transfer at low frequency were observed.

Acknowledgements

The authors acknowledge the support for this work from Indiana University Kokomo.

Conflicts of Interest

The authors declare that they have no known competing financial interests or personal relationships that could have appeared to influence the work reported in this paper.

References

[1] Sun, S., Fan, E., Xu, H., Cao, W., Shao, G., Fan, B., *et al.* (2019) Enhancement of Photocatalytic Activity of g-C_3N_4 by Hydrochloric Acid Treatment of Melamine. *Nanotechnology*, **30**, Article ID: 315601. https://doi.org/10.1088/1361-6528/ab10fd

[2] Wang, X., Maeda, K., Thomas, A., Takanabe, K., Xin, G., Carlsson, J.M., *et al.* (2008) A Metal-Free Polymeric Photocatalyst for Hydrogen Production from Water under Visible Light. *Nature Materials*, **8**, 76-80. https://doi.org/10.1038/nmat2317

[3] Huai, X., Hang, Z., Wang, Z., Liu, D., Li, Q., He, Z., *et al.* (2018) Efficiently Enhancing the Photocatalytic Activity of g-C_3N_4 by a Simple Advanced Successive Activation Method. *Micro & Nano Letters*, **13**, 403-406. https://doi.org/10.1049/mnl.2017.0518

[4] Khezami, L., Ben Aissa, M.A., Modwi, A., Ismail, M., Guesmi, A., Algethami, F.K., Ben Ticha, M., Assadi, A.A. and Nguyen-Tri, P. (2022) Harmonizing the Photocatalytic Activity of g-C_3N_4 Nanosheets by ZrO_2 stuffing: From Fabrication to Experimental Study for the Wastewater Treatment. *Biochemical Engineering Journal*, **182**, Article ID: 108411.

[5] Li, R., Wang, B. and Wang, R. (2023) Photocatalytic Activities of g-C_3N_4 (CN) Treated with Nitric Acid Vapor for the Degradation of Pollutants in Wastewater. *Materials*, **16**, Article 2177. https://doi.org/10.3390/ma16062177

[6] Ouyang, H.B., Huang, J.F., Zeng, X.R., Cao, L.Y., Li, C.Y., Xiong, X.B. and Jie, F. (2014) Visible-Light Photocatalytic Activity of SiC Hollow Spheres Prepared by a Vapor-Solid Reaction of Carbon Spheres and Silicon Monoxide. *Ceramics International*,

40, 2619-2625.

[7] Lu, W., Guo, L., Jia, Y., Guo, Y., Li, Z., Lin, J., *et al.* (2014) Significant Enhancement in Photocatalytic Activity of High Quality SiC/Graphene Core-Shell Heterojunction with Optimal Structural Parameters. *RSC Advances*, **4**, 46771-46779. https://doi.org/10.1039/c4ra06026a

[8] García-Muñoz, P., Fresno, F., Lefevre, C., Robert, D. and Keller, N. (2020) Ti-Modified $LaFeO_3$/β-Sic Alveolar Foams as Immobilized Dual Catalysts with Combined Photo-Fenton and Photocatalytic Activity. *ACS Applied Materials & Interfaces*, **12**, 57025-57037. https://doi.org/10.1021/acsami.0c16647

[9] Wang, Y., Zhang, L., Zhang, X., Zhang, Z., Tong, Y., Li, F., *et al.* (2017) Openmouthed B-Sic Hollow-Sphere with Highly Photocatalytic Activity for Reduction of CO_2 with H_2O. *Applied Catalysis B*: *Environmental*, **206**, 158-167. https://doi.org/10.1016/j.apcatb.2017.01.028

[10] Liu, Y., Wang, B., Li, D., Shen, J., Zhang, Z. and Wang, X. (2022) Fabrication of 2H/3C-SiC Heterophase Junction Nanocages for Enhancing Photocatalytic CO_2 Reduction. *Journal of Colloid and Interface Science*, **622**, 31-39. https://doi.org/10.1016/j.jcis.2022.04.111

[11] Su, Y., Chen, P., Wang, F., Zhang, Q., Chen, T., Wang, Y., *et al.* (2017) Decoration of TiO_2/g-C_3N_4 Z-Scheme by Carbon Dots as a Novel Photocatalyst with Improved Visible-Light Photocatalytic Performance for the Degradation of Enrofloxacin. *RSC Advances*, **7**, 34096-34103. https://doi.org/10.1039/c7ra05485h

[12] Guo, F., Shi, W., Guan, W., Huang, H. and Liu, Y. (2017) Carbon Dots/g-C_3N_4/ZnO Nanocomposite as Efficient Visible-Light Driven Photocatalyst for Tetracycline Total Degradation. *Separation and Purification Technology*, **173**, 295-303. https://doi.org/10.1016/j.seppur.2016.09.040

[13] Asadzadeh-Khaneghah, S., Habibi-Yangjeh, A., Shahedi Asl, M., Ahmadi, Z. and Ghosh, S. (2020) Synthesis of Novel Ternary g-C_3N_4/SiC/C-Dots Photocatalysts and Their Visible-Light-Induced Activities in Removal of Various Contaminants. *Journal of Photochemistry and Photobiology A*: *Chemistry*, **392**, Article ID: 112431. https://doi.org/10.1016/j.jphotochem.2020.112431

[14] Wang, B., Zhang, J.T. and Huang, F. (2017) Enhanced Visible Light Photocatalytic H_2 Evolution of Metal-Free g-C_3N_4/SiC Heterostructured Photocatalysts. *Applied Surface Science*, **391**, 449-456.

[15] Kasem, K.K., Pu, J. and Cox, L. (2023) Photoactivities of Thiophene Monomer/Polymer Transition in Gel-Based Photoelectrochemical Assembly: A Theoretical/Experimental Approach. *International Journal of Electrochemical Science*, **18**, Article ID: 100077. https://doi.org/10.1016/j.ijoes.2023.100077

[16] Wu, J.H., Hao, S.C., Lan, Z., Lin, J.M., Huang, M.L., Huang, Y.F., *et al.* (2007) A Thermoplastic Gel Electrolyte for Stable Quasi-Solid-State Dye-Sensitized Solar Cells. *Advanced Functional Materials*, **17**, 2645-2652. https://doi.org/10.1002/adfm.200600621

[17] Guo, H., Gao, S., Chai, X., Shi, Y. and Gao, J. (2023) Preparation of Z-Type Heterojunction SiCf/g-C_3N_4 Composites with Enhanced Photocatalytic Degradation of Tetracycline under Visible Light. *Applied Organometallic Chemistry*, **37**, e7022. https://doi.org/10.1002/aoc.7022

[18] Spadavecchia, F., Ardizzone, S., Cappelletti, G., Falciola, L., Ceotto, M. and Lotti, D. (2012) Investigation and Optimization of Photocurrent Transient Measurements on Nano-TiO_2. *Journal of Applied Electrochemistry*, **43**, 217-225. https://doi.org/10.1007/s10800-012-0485-2

[19] Roslan, S.A., Md Sabri, A.A., Roslan, N.A., Bawazeer, T.M., Alsoufi, M.S., Aziz, F., *et al*. (2024) Equal Proportion of Donor/Acceptor Active Layer for Reduced Dark Current in Visible Organic Photodiode. *Optical Materials*, **147**, Article ID: 114781. https://doi.org/10.1016/j.optmat.2023.114781

[20] Keiser, H., Beccu, K.D. and Gutjahr, M.A. (1976) Abschätzung der porenstruktur poröser elektroden aus impedanzmessungen. *Electrochimica Acta*, **21**, 539-543. https://doi.org/10.1016/0013-4686(76)85147-x

[21] Kasem, K., Masuda, H. and Mendez Rodriguez, A. (2024) Tracking the Photoactivity at the Interface of SiC/Poly 2(2-Thienyl) Furan Thin Solid Film in Polymer Gel Electrolytes. *Journal of Electrochemical Science and Engineering*, **14**, 671-684. https://doi.org/10.5599/jese.2401